

Phase Separation of Poly(*N*-isopropylacrylamide) in Water: A Spectroscopic Study of a Polymer Tagged with a Fluorescent Dye and a Spin Label

Françoise M. Winnik*

Xerox Research Center of Canada, 2660 Speakman Drive, Mississauga Ontario, Canada L5K 2L1

M. Francesca Ottaviani

Dipartimento di Chimica, Università di Firenze, Via Gino Capponi 9, 50121 Firenze, Italy

Stefan H. Bossman,[†] Wenseng Pan, M. Garcia-Garibay,[‡] and Nicholas J. Turro*

Department of Chemistry, Havemeyer Hall, Columbia University, New York, New York 10027

Received: July 19, 1993; In Final Form: September 22, 1993*

A spin label (4-amino-2,2,6,6-tetramethylpiperidine 1-oxide, TEMPO) and a fluorescence dye (1-pyrenylbutyl, Py) were attached randomly along the same poly(*N*-isopropylacrylamide) chain (PNIPAM-Py-T, M_v , 2.3×10^6 , Py content 1.9×10^{-5} mol g⁻¹), and their interactions in solutions of the polymer were studied using electron paramagnetic resonance (EPR), ¹³C nuclear magnetic resonance (¹³C NMR), and fluorescence spectroscopy. The thermoreversible phase transition of aqueous solutions of the polymer was examined by these three techniques. EPR spectra of solutions of PNIPAM-Py-T (3 g L⁻¹) were recorded as a function of temperature (20–35 °C) and analyzed in terms of the isotropic hyperfine coupling constant and the correlation time for the reorientation motion. The temperature dependence of the simulated spectra. The fluorescence of PNIPAM-Py-T in cold water (1 g L⁻¹) displayed contributions from isolated excited pyrenes (Py*, monomer emission) and from preassociated pyrenes ("excimer" emission). This excimer emission decreased at the phase transition temperature while the monomer emission increased. Quantum yield determinations and fluorescence lifetime measurements are interpreted in terms of two competing temperature-induced effects: (1) a disruption of the pyrene preassociation and (2) an increase in the efficiency of the quenching of Py* by the TEMPO nitroxide radicals. Supporting evidence was obtained by fluorescence measurements carried out with solutions of PNIPAM-Py-T in methanol and by intermolecular fluorescence quenching experiments using a singly labeled polymer (PNIPAM-Py, M_v , 2.6×10^6 , Py content 4.2×10^{-5} mol g⁻¹) and either TEMPO or a TEMPO-labeled polymer (PNIPAM-T, M_v , 2.9×10^6 , TEMPO content 1×10^{-5} mol g⁻¹).

Introduction

The growth of the biotechnology field over the past decade has created a demand for new materials capable of performing a controlled function in response to an external stimulus, such as a flash of light, an electrical impulse, or a temperature jump. Thermosensitive polymers which demonstrate good solubility in water at low temperature but separate from solution when the temperature is raised can be employed to perform such tasks. For practical reasons it is often necessary to crosslink these polymers to create hydrogels which have been used in applications, such as controlled drug delivery¹ and solute separation.² The design of performing thermosensitive gels requires an understanding of detailed aspects of the temperature-induced expansion and contraction of the network. The temperature-induced phase-separation experienced by some aqueous polymer solutions provides an excellent model to study the molecular interactions at play in thermoreversible hydrogels.³ Aqueous solutions of poly(*N*-isopropylacrylamide) (PNIPAM, Figure 1) exhibit this reverse temperature phase behavior, with a cloud point at 31 °C.⁴ The solubility of the polymer in cold water can be attributed to its ability to form H bonds with water via the amide groups while inducing considerable ordering of the solvent through the apolar isopropyl substituents. This water structuring brings about large negative contributions to both the enthalpy ΔH_M and the entropy ΔS_M of mixing. At a sufficiently high temperature the entropic

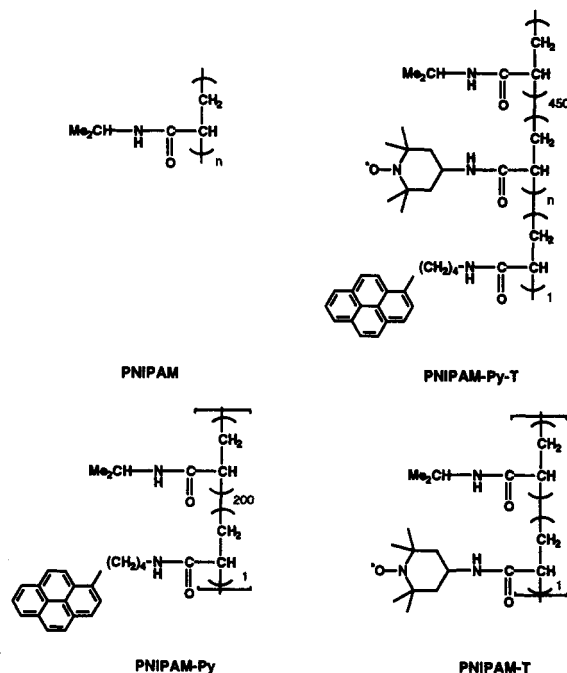


Figure 1. Structure of the polymers used in this study.

term of the free energy of mixing will overcome the negative enthalpy of solution, resulting in a positive free energy. Thus at this temperature phase separation occurs.

The macroscopic phase separation reflects the collapse of individually solvated coils into dehydrated globules which ag-

* Present address: Universität Karlsruhe, Engler-Bunte Institut, Richard Willstätter Allee 5, D-W-7500 Karlsruhe 1, Germany.

[†] Present address: Department of Chemistry, University of California in Los Angeles, 405 Hilgard Ave., Los Angeles, CA 90024.

• Abstract published in *Advance ACS Abstracts*, November 15, 1993.

gregate to form a polymer-rich phase insoluble in water. This detailed mechanistic description has evolved from the merging of data gathered from calorimetric determinations,⁵ light-scattering measurements,⁶ fluorescence,^{7,8} Raman, EPR, and NMR spectroscopy.⁹ Each technique has its limitations and poses its intrinsic ambiguities during data interpretation. Therefore it may be important to scrutinize a polymer by several spectroscopic tools. In this way different distance scales or time domains can be probed to generate a more global description.

The work described here originates from our previous investigations of the use of fluorescence,^{7,10} electron paramagnetic resonance (EPR),^{11,12} and cross-polarization ¹³C magic angle spinning nuclear magnetic resonance¹¹ (CP MAS NMR) polymers in water. The fluorescence studies^{7,10} relied primarily on the photophysical properties of the pyrene label attached randomly along the poly(*n*-isopropylacrylamide) backbone (PNIPAM-Py, Figure 1). The emission of this polymer in cold water is characterized by a strong contribution from pyrene excimers originating from preassociated pyrenes. At the cloud point the pyrene excimer emission decreases rapidly with a concomitant increase of the emission from isolated pyrenes (pyrene monomer emission), revealing the heat-induced disruption of the pyrene aggregates formed in cold water. The EPR investigations^{11,12} were based on polymers tagged randomly with 2,2,6,6-tetramethylpiperidine 1-oxide (TEMPO, PNIPAM-T; see Figure 1). The EPR spectrum of this polymer in cold water consists of a major component (signal B) and of a minor contributor (signal A) associated with a faster motion of the probe. At the phase transition a new signal (component C) grows in at the expense of signal B. This new component is characterized by a much longer correlation time of motion than component B, indicating a decrease in the mobility of the probe in the separated polymer-rich phase. Both the fluorescence spectra and the EPR signals recovered their original features when the aqueous polymer mixtures were cooled below their cloud point, emphasizing the reversibility of the phase separation.

Nitroxide radicals act as good quenchers of the excited electronic states of a wide variety of fluorescent molecules.¹³ These effects take place intermolecularly in solutions of low molecular weight probes as well as intramolecularly in molecules consisting of a chromophore linked to a nitroxide radical.¹⁴ Recently, fluorescence quenching by nitroxides has become an important tool with which to probe the structural and dynamic properties of membranes,¹⁵ micelles,¹⁶ and proteins in solution.¹⁷ We report here that the same spectroscopic techniques can be used to study the interactions among fluorescent dyes and nitroxide radicals attached to the same polymer chain. We prepared a polymer (PNIPAM-Py-T, Figure 1) carrying both a fluorescent dye, pyrene (Py), and an EPR label, TEMPO. Cross-polarization magic angle spinning ¹³C NMR spectra, EPR spectra, and fluorescence spectra were recorded from solutions of this polymer in water below and above the cloud point. Complementary fluorescence experiments were carried out (1) with solutions of this polymer in methanol, and (2) with aqueous solutions of pyrene-labeled poly(*N*-isopropylacrylamide) in the presence of an EPR probe (TEMPO) and in the presence of a TEMPO-labeled polymer. The objectives of the study were to assess the role of the polymer backbone on the interactions between the two labels and to gain further insight into the mechanism of the phase transition and the composition of the anisotropic mixture formed above the cloud point.

Experimental Section

Materials. All commercial chemicals were purchased from Aldrich Chemical Co., unless otherwise noted. *N*-Isopropylacrylamide was purchased from Eastman Kodak Chemicals. The EPR probes 2,2,6,6-tetramethylpiperidine 1-oxide (TEMPO) and 4-amino-2,2,6,6-tetramethylpiperidine 1-oxide (4-aminoTEMPO) were used without purification. Water was deionized with

a Millipore Milli-Q water purification system. HPLC grade solvents were used for all spectroscopic measurements. For the syntheses, reagent-grade solvents were used without further purification, except for tetrahydrofuran (THF), which was dried by distillation from sodium benzophenone. The reactive polymer, *N*-isopropylacrylamide/*N*-(acryloxy)succinamide copolymer, (PNIPAM-NASI) was prepared by free-radical copolymerization of *N*-isopropylacrylamide and *N*-(acryloxy)succinimide in *tert*-butyl alcohol, as described previously.¹⁰

Preparation of Labeled Poly(*N*-isopropylacrylamides).
PNIPAM-T. This singly labeled polymer was prepared by reaction of 4-amino-2,2,6,6-tetramethylpiperidine 1-oxide with a copolymer of *N*-isopropylacrylamide and *N*-(acryloxy)succinimide (PNIPAM-NASI), as described previously.¹¹ The TEMPO content in this polymer was 9.8×10^{-6} mol g⁻¹ or 1 TEMPO group/880 monomer units (PNIPAM-T/880).

PNIPAM-Py-T. A solution of PNIPAM-NASI (1.0 g) and 4-amino-2,2,6,6-tetramethylpiperidine 1-oxide (6.0 mg, 3.5×10^{-5} mol, 4-amino-TEMPO) in dry THF was stirred at room temperature in the dark and under nitrogen for 17 h. To the reaction mixture were added first a solution of 4-(1-pyrenyl)butylammonium hydrochloride (5.0 mg, mol)¹⁸ in THF (2 mL) and then triethylamine (0.2 mL). Stirring at room temperature was continued for 24 h. Isopropylamine (0.1 mL) was added to the reaction mixture to quench the unreacted *N*-oxysuccinimido groups. The mixture was stirred for 3 h after the addition. The polymer was isolated by precipitation into hexane (300 mL). It was purified by two precipitations of dioxane solutions (10 mL) into diethyl ether (250 mL). The separated polymer was dried in vacuo for 24 h at 40 °C (0.950 g). It was redissolved in water and isolated by freeze-drying; UV (methanol) λ_{\max} 265, 275, 312, 326, and 342 nm. The purity of the polymer was ascertained by GPC analysis, which indicated the absence of low molecular weight impurities and that the chemical transformation did not alter the (broad) molecular weight distribution of the polymer. The amount of pyrene attached to the polymer was determined by UV analysis of solutions of the polymer in methanol, using as reference compound 4-(1-pyrenyl)butylamine hydrochloride (λ_{\max} 342 nm, $\epsilon = 32\,800$).¹⁹ The TEMPO content could not be calculated from UV data because of interference from the absorption of pyrene. It was estimated to be ca. $(2-3) \times 10^{-5}$ mol g⁻¹ of polymer by comparison of the intensity of the EPR signal of the nitroxide label in a sample of the polymer solution (MeOH, 20 °C) to that of the EPR signal of a probe (4-amino-TEMPO) in the same solvent. Viscosity-averaged molecular weights were calculated from the intrinsic viscosity $[\eta]$ of the polymer in THF solution, using the viscometric relationship: $[\eta] = 9.59 \times 10^{-3} M^{0.65}$ cm³ g⁻¹.²⁰ Pyrene content 1.9×10^{-5} mol g⁻¹, or 1 pyrene/400 NIPAM units; TEMPO content 9.8×10^{-6} mol g⁻¹ or 1 TEMPO/450 NIPAM units, PNIPAM-Py/400-T/450 (Table I).

Instrumentation. UV spectra were recorded with a Varian UV-VIS-NIR Cary-5 spectrophotometer. Solution viscosities were measured at 30 °C with a Viscotek Model 100 differential viscometer (THF, temperature 30 °C, polymer concentration ca. 75 ppm). Gel permeation chromatography (GPC) measurements were performed with a Waters WISP 700 system equipped with a Waters RI 410 refractive index detector. Four ultrastyrigel columns (10 000, 5000, 500, and 100 Å) were used. The eluent (THF) was used at a flow rate of 0.8 mL min⁻¹. Polystyrene standards were used to determine molecular weights and molecular weight distributions. Cloud points were determined by spectrophotometric detection of changes in turbidity of solutions (1 g L⁻¹) heated at a constant rate (0.2 °C min⁻¹) in a magnetically stirred UV cell, as described previously. ¹³C CP MAS NMR spectra were recorded at a field of 62.8 MHz with a Bruker AF 250 spectrometer equipped with a solid-state probe manufactured by Dotty Scientific, using decoupling RF fields with γB_{1H} of ca.

TABLE I: Physical Properties of the Polymers

polymer	$[\eta]^a$ (cm ³ g ⁻¹)	$M_{\text{viscosity}}^b$	M_n^c	M_w^c	LCST (1 g L ⁻¹) (°C)	[Py] (mol g ⁻¹)	[Tempo] (mol g ⁻¹)
PNIPAM	72 ± 1	0.92 × 10 ⁶	55 000	120 000	32.5		
PNIPAM-NASI	414 ± 3	2.6 × 10 ⁶	87 000	340 000	32.4		
PNIPAM-T	151 ± 3	2.9 × 10 ⁶	90 000	340 000	32.2		1 × 10 ⁻⁵
PNIPAM-Py	141 ± 3	2.6 × 10 ⁶	87 000	340 000	32.4	4.2 × 10 ⁻⁵	
PNIPAM-Py-T	131.8 ± 3	2.3 × 10 ⁶	85 800	360 000	31.2	1.9 × 10 ⁻⁵	<i>d</i>

^a From THF solutions. ^b From $[\eta] = 9.59 \times 10^{-3} M_v$ (see ref 20). ^c GPC in THF, calibrated against polystyrene standards. ^d Could not be determined by absorption spectroscopy.

40 kHz. The Hartmann–Hahn condition was adjusted to obtain best resolution. Chemical shifts were calibrated with a sample of *p*-di-*tert*-butylbenzene [$\delta(\text{CH}_3)_3 = 31$ ppm]. Contact times for cross-polarization were optimized for maximum signal between 100 and 2000 ms and recycle delays were 2–4 s. Samples of solid and dissolved polymer were placed in a 7-mm-i.d. sapphire rotor with O-ring sealed macor caps. The samples were spun at the magic angle at 3 ± 0.25 kHz. EPR spectra were recorded with a Bruker ESP 300 spectrometer with an ESP 1600 data analysis software. Temperature control ($T \pm 1$ °C) was achieved with a Bruker ER 4111T variable temperature accessory. Steady-state fluorescence spectra were recorded with SPEX fluorescence spectrometers (DM1B or DM212) equipped with a DM2000F data analysis program. Time-resolved fluorescence measurements were performed with a single-photon-counting unit consisting of a 199F nanosecond flash lamp from Edinburgh Instruments Inc., Ortec electronics, and a Tracor-Northern TN-1710 multichannel analyzer interfaced to an IBM PS/2 Model 70 computer. Decay traces were analyzed with a computer program generously provided by Professor F. C. DeSchryver (University of Leuven, Belgium).

Analysis of the EPR Spectra. In the case of labeled polymers, the analysis of the signals was performed by using the procedure reported by Schneider and Freed.²¹ This procedure is particularly well suited for the analysis of signals originating from nitroxides in slow motion conditions, i.e., correlation times for rotational diffusion between 5×10^{-7} and $(1-2) \times 10^{-9}$ s. Best fits were obtained by setting parameters such as (1) the input magnetic parameters for the *g* and *A* tensor components (for the Zeeman and hyperfine interactions, respectively) were evaluated by computing the spectra in the slowest motion, i.e., at liquid nitrogen temperature, (2) the model for the rotational diffusion motion (Brownian motion, free motion, or jump motion), and (3) the principal components of the diffusion tensor. In the computation of the EPR spectra, the simulations included the tilt angle of the rotational diffusional axes with respect to the magnetic molecular axes. In this case the simulations yielded an exact *N* value ($N = D_{\parallel}/D_{\perp}$, where D_{\parallel} and D_{\perp} are the parallel and perpendicular components of the rotational diffusional tensor). For these calculations the following parameters were employed (aqueous solutions): *g* components: $g_{xx} = 2.0087$, $g_{yy} = 2.0064$, $g_{zz} = 2.0038$; *A* components: $A_{xx} = 6.5$ G, $A_{yy} = 7.5$ G, $A_{zz} = 36.5$ G; $N = 4$ ($N = D_{\parallel}/D_{\perp}$); tilt angles: component *A*: 90°, component *B*: 30°, component *C*: 0° $z' = z$ axis, corresponding to the direction of the *p*_z orbital containing the unpaired electron. In cases where more than one signal contributed to the EPR spectra, each signal was computed separately and added in a ratio appropriate to simulate the experimental spectrum. A subtraction–addition procedure was performed in order to identify the spectrum line shapes. The accuracies in the determination of rotational correlation times were $\pm 10\%$ and ± 0.05 G in the determination of rotational correlation times were $\pm 10\%$ and ± 0.05 G in the determination of hyperfine coupling constants.

Preparation of Samples for EPR and NMR Analysis. Solutions of the labeled polymers for EPR analysis were prepared by dissolving the polymers (4 g L⁻¹) in water or methanol. Adequate time (ca. 24 h at room temperature) was allowed to ensure complete dissolution of the polymers in water. Solutions in methanol were degassed by a 20-min purge with argon. The

conditions for very effective degassing procedure were adjusted using a method based on the determination of the biacetyl fluorescence to photophorescence emission.²² For NMR analysis the polymer concentration was 10 g L⁻¹.

Fluorescence Measurements. Lifetime measurements were performed with an excitation wavelength of 332 nm. The emission was monitored at 380 nm (monomer lifetimes) or 480 nm (excimer lifetimes) unless otherwise specified. For steady-state emission measurements the excitation wavelength was 332 nm. Excitation and emission slit widths were set at 6 and 1 mm, respectively. Excitation spectra recorded in the ratio mode were monitored at 396 nm (monomer emission) and 480 nm (excimer emission). The concentrations of the polymer solutions were 1 g L⁻¹. They were prepared by dilution of a stock solution (4 g L⁻¹) and kept at room temperature for 12 h prior to analysis. Solutions in methanol were degassed either by a 20-min bubbling with argon or by freeze–thaw cycles. Measurements carried out with samples degassed by the two techniques yielded identical results. Quantum yields were calculated by integration of peak areas of corrected spectra in wavenumber units, using as standard quinine sulfate in 1 N H₂SO₄ ($\phi = 0.546$, $\lambda_{\text{exc}} = 328$ nm, 25 °C).²³ Beer's law corrections were applied for optical density changes at the excitation wavelength. Corrections were made as well to account for refractive indexes differences. The excimer-to-monomer emission ratio was calculated by taking the ratio of the emission intensity at 480 nm (peak height) to the half-sum of the emission intensities at 378 and 396 nm.

Solutions for Fluorescence Quenching Experiments. Solutions of PNIPAM-Py (60 ppm) in water and in methanol were prepared from well-equilibrated stock solutions (1 g L⁻¹). For the experiments with TEMPO, samples of desired TEMPO concentration were obtained by addition of freshly prepared solutions of TEMPO (5×10^{-2} mol L⁻¹) in methanol or in water to the polymer solutions. For the experiments with PINIPAM-T/880, samples of desired nitroxide label concentration were prepared by addition of aliquots of a well-equilibrated solution of PNIPAM-T in water (12.5 g L⁻¹, [TEMPO] = 1.25×10^{-4} mol L⁻¹) to solutions in water of PNIPAM-Py/200 (60 ppm) and PNIPAM, the concentration of the later polymer was adjusted to keep the total polymer concentration (2.5 g L⁻¹) constant throughout the samples. Solutions in methanol were degassed by vigorous bubbling with methanol-saturated argon. For measurements above the LCST aqueous solutions of the polymer containing a given amount of quencher were heated to 35 °C in the spectrometer cell holder. They were kept at this temperature for 20 min. After this time their spectrum was recorded at 35 °C.

Results and Discussion

Attachment of the EPR and fluorescence labels to the PNIPAM backbone was achieved by reacting a copolymer of *N*-isopropylacrylamide and *N*-(acryloxy)succinimide (PNIPAM-NASI), first with 4-amino-2,2,6,6-tetramethylpiperidinoxyl (4-amino-TEMPO), then with (4-(1-pyrenyl)butyl)ammonium hydrochloride, and finally with *N*-isopropylamine, to quench any unreacted acryloxysuccinimido moieties (Figure 2). The polymer was purified by repeated reprecipitations to ensure the absence of unreacted fluorescent dye and of 4-amino-TEMPO. It was characterized by the standard techniques (Table I).

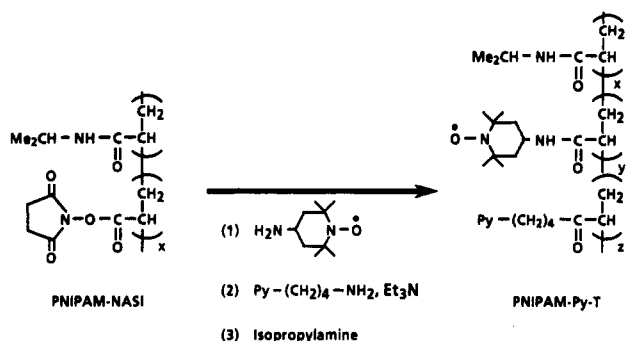


Figure 2. Synthetic scheme for the preparation of TEMPO- and pyrene-dilabeled poly(*N*-isopropylacrylamide).

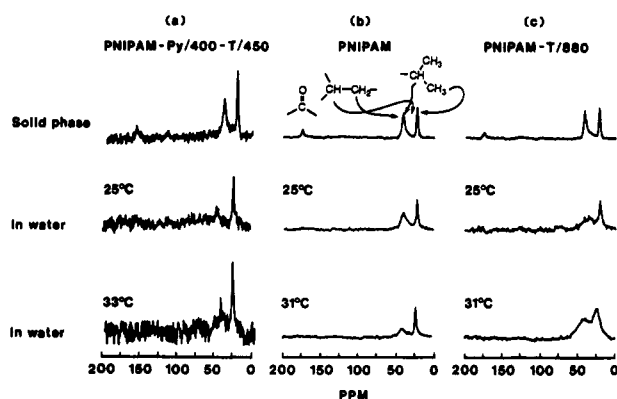


Figure 3. ^{13}C CP-MAS NMR spectra of (a) PNIPAM-Py-T, (b) PNIPAM, and (c) PNIPAM-T in the solid phase, and in cold water solutions and above the cloud point.

(1) CP-MAS ^{13}C NMR Spectroscopy. Cross-polarization magic angle spinning (CP-MAS) ^{13}C NMR spectra of PNIPAM-Py-T were recorded for aqueous solutions below and above the LCST and for the polymer in the solid phase (Figure 3a). The spectrum of the polymer powder exhibited a signal at 160 ppm, assigned to the carbon of the carbonyl group of the pendent isopropylacrylamides and two signals at 42 and 25 ppm attributed to the isopropyl methine and methyl carbons, respectively. The signals due to the backbone methine and methylene carbons were unresolved, contributing as weak shoulders to the signal centered at 42 ppm. For aqueous solutions of the polymer all the signals lost their sharpness and the signal due to the carbonyl carbon could not be detected. Within the limits of the signal to noise ratio, it appears that the signals in spectra above the LCST experience some broadening as compared to those recorded from cold solutions. The line broadening may be indicative of the decreased mobility of the isopropyl carbons in the phase separated polymer. This is also observed in the corresponding spectra of unlabeled poly(*N*-isopropylacrylamide) (Figure 3b).⁹ Such effects have been reported also in a recent NMR study of the phase transition in aqueous solutions of cellulose ethers.²⁴

Also shown in Figure 3 are the temperature-dependent spectra of an aqueous solution of the polymer PNIPAM-T labeled only with nitroxide groups. This polymer, (Figure 1) carries on average 1 TEMPO label/880 monomer units; hence its degree of labeling is about half that of PNIPAM-Py-T. For this singly labeled polymer the broadening of the methine and methylene signals in spectra recorded above the LCST of the solutions was much more pronounced.¹¹ It is well-known that free radicals can cause shifts in resonance frequencies, decreases in relaxation times, or broadening of line widths.²⁵ The magnitude of the effects depends on the amount of nitroxide groups attached to the polymer and on the chain conformation and mobility of the polymer. We attributed the loss of resolution and of intensity in the spectra of PNIPAM-T to the occurrence of strong interactions between the nitroxide groups and isopropyl carbons in the phase-separated

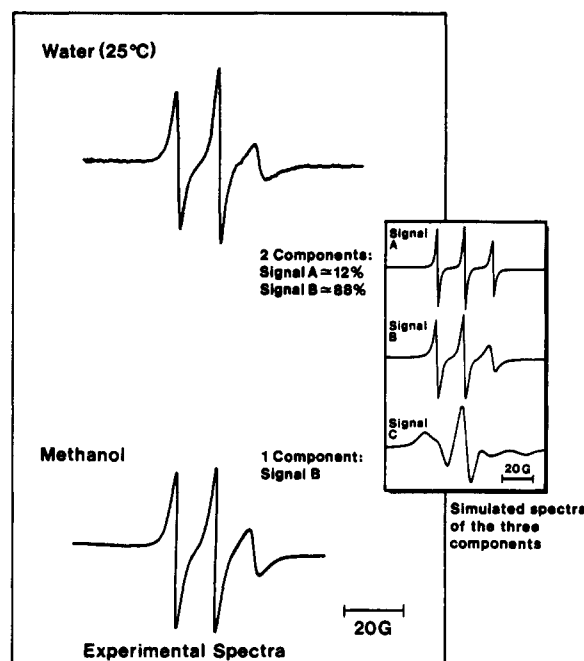


Figure 4. EPR spectra of pyrene- and TEMPO-dilabeled poly(*N*-isopropylacrylamide) (PNIPAM-Py-T) in water and in methanol; 25 °C, polymer concentration 4 g L⁻¹. Inset: simulated EPR signals of the three components A, B, and C employed in the analysis of the EPR spectra of TEMPO-labeled polymers.

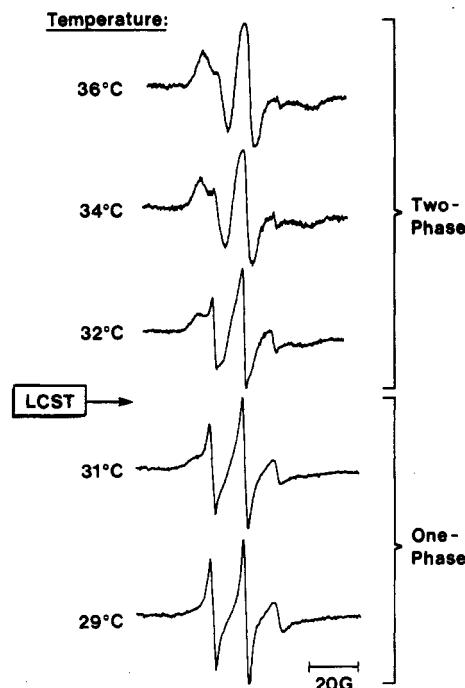
polymer. The contrasting observations in the ^{13}C NMR spectra of PNIPAM-Py-T reveal significant differences in the motion of the nitroxide group in the time scale probed by the NMR measurements. Sharp and broad components rather than a time-averaged spectrum above the LCST argue in favor of inhomogeneities in the polymer-rich phase. These may be also induced by the hydrophobic fluorophores also attached on the polymer chain.

(2) EPR Spectroscopy. The EPR spectra of TEMPO-labeled poly(*N*-isopropylacrylamides) exhibit the typical three-line pattern due to coupling of the electronic spin of the nitroxide function with the nuclear spin ($I = 1$) of the ^{14}N nucleus. EPR line shapes are usually analyzed by taking into account mobility and structural parameters to solve the spin Hamiltonian and the relaxation matrix. Among the various parameters which can be extracted from a spectral analysis the most useful in characterizing a system are the components of the hyperfine coupling tensor, the G factor, the line widths, and the correlation times for rotational motion. The correlation times for motion provide information of the local mobility of the probe. Under conditions of highly anisotropic motion, as for example in the case of the nitroxide group of PNIPAM-Py-T in methanol (Figure 4), it is possible to determine the correlation times for the motion of the probe in different directions. Thus, the analysis of this spectrum which takes into account the tilt of the main rotational axis toward the N-O direction ($z' = x$) indicates a rather fast mobility of the probe along the N-O direction ($\tau_c = 9.9 \times 10^{-11}$ s) and a much slower motion ($\tau_c = 5 \times 10^{-9}$ s) in the perpendicular direction. This is an indication of the restriction of motion experienced by a nitroxide group attached to the PNIPAM chain. The value of τ_c (7×10^{-10} s) reported in Table II represents an average over all directions. In conditions of fast motion ($\tau_c < (1-2) \times 10^{-9}$ s) the anisotropies are averaged to zero and the isotropic hyperfine coupling constant (A_N) can be used. It becomes an extremely valuable parameter which reveals changes in the polarity of the microenvironment experienced by the nitroxide.

The spectrum of PNIPAM-Py-T in water consisted of more than one component (Figure 4). It was computed as a sum of several signals and the different percent contribution of each spectral component was evaluated, adopting the following

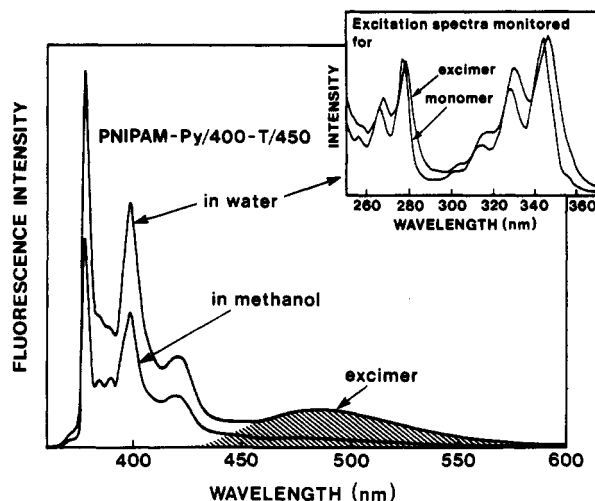
TABLE II: EPR Spectral Characteristics^a of PNIPAM-Py-T^b in Water, THF, and in Methanol

	water		MeOH	
	25 °C	33 °C	25 °C	35 °C
$\tau_C(A)$ (s)	2×10^{-10}	2×10^{-10}		
$\tau_C(A)$ (%)	12	10		
$\langle A_N \rangle$ (G)	17.0	17.0		
$\tau_C(B)$ (s)	1.5×10^{-9}	1.0×10^{-9}	7×10^{-10}	5×10^{-10}
$\tau_C(B)$ (%)	88	8	100	100
$\langle A_N \rangle$ (G)	16.8	16.9	16.4	
$\tau_C(C)$ (s)		8.0×10^{-9}		
$\tau_C(C)$ (%)		82		
$A'_{zz}(G)$		63		

^a τ_C = rotational correlation time; $\langle A_N \rangle$ = hyperfine coupling constant.^b Polymer concentration 1 g L⁻¹.**Figure 5.** Experimental EPR spectra of pyrene- and TEMPO-dilabeled poly(*N*-isopropylacrylamide) (PNIPAM-Py-T) in water at several temperatures; polymer concentration 4 g L⁻¹.

procedure. First, a subtraction-addition routine was used to identify each component. Then, magnetic and mobility parameters were calculated by the spectral simulation method developed by Schneider and Freed,²¹ assuming Lorentzian line shape of the signal, isotropic motion of the label, and choosing as magnetic parameters those reported for 4-amino-TEMPO in water. With these assumptions the EPR signals of PNIPAM-Py-T in water (25 °C) were analyzed as a sum of two components: a major component (B, $\tau_C \approx 1.5 \times 10^{-9}$ s) and a minor component associated with a faster motion of the label (A, $\tau_C \approx 2 \times 10^{-10}$ s). The spectrum of PNIPAM-Py-T in methanol consisted of only one component (B, $\tau_C \approx 7 \times 10^{-10}$ s). These correlation times of motion are much slower than that of the free probe 4-amino-TEMPO ($\tau_C \approx (1-6) \times 10^{-11}$ s, in water),²⁶ confirming that the nitroxide group is indeed attached to the polymer chain.

Next we monitored the effects of changes in solution temperature of the spectra of the labeled polymer in water. Dramatic changes in the EPR spectrum of PNIPAM-Py-T occurred as the solution was heated through its LCST (Figure 5). Most significant was the sudden growing-in at the expense of component B of a new signal (component C) characterized by a much longer correlation time ($\tau_C = 8.0 \times 10^{-9}$ s, 33 °C). The heat-induced changes were reversible. Upon cooling, component B appeared at the expense of C, as the temperature dropped below the LCST. The minor contributor, component A, did not respond to a

**Figure 6.** Fluorescence spectra of the pyrene- and TEMPO-dilabeled poly(*N*-isopropylacrylamide) (PNIPAM-Py/400-T/450) in water and in methanol. Temperature 25 °C, polymer concentration 0.06 g L⁻¹, $\lambda_{exc} = 331$ nm. Inset: excitation spectra of the polymer in water monitored for the excimer and monomer emissions.**TABLE III: Photophysical Parameters of the Labeled Polymers**

parameter	PNIPAM-Py-T		PNIPAM-Py ¹⁰	
	H ₂ O	MeOH	H ₂ O	MeOH
I_E/I_M	0.15	<0.02	0.45	0.10
λ_E (nm)	480	485	480	485
$\Delta\lambda$ (nm)	2	0	2	0
P_M	2.35	2.5	1.8	2.5
P_E	1.7	2.5	2.2	2.5

significant extent to these changes in temperature. The overall features of the EPR spectra of the doubly labeled polymer agree well with those reported for the labeled polymer carrying only nitroxide tags, PNIPAM-T.¹¹ Only slight discrepancies were detected, such as differences in the calculated correlation times for motion of component B: $\tau_C(B) = 1.0 \times 10^{-9}$ s in PNIPAM-T/880,¹ vs $\tau_C(B) = 1.5 \times 10^{-9}$ s for PNIPAM-Py/400-T/450. The insensitivity of the TEMPO label to the presence of pyrene chromophores is in sharp contrast to the influence of this nitroxide group on the fluorescence of pyrene, as described in the next section.

(3) Photophysical Studies. Spectroscopy of a TEMPO/Pyrene-Dilabeled Poly(*N*-isopropylacrylamide). The spectrum of PNIPAM-Py-T dissolved in cold water presented an emission originating from locally excited Py (intensity I_M , monomer emission) with the (0,0) band located at 378 nm together with a broad featureless emission centered at 480 nm associated with pyrene excimers (intensity I_E ; Figure 6). The total fluorescence quantum yield of the pyrene emission ($\phi_f = 0.45$) was only slightly lower than that of PNIPAM-Py in water ($\phi_f = 0.52$). Analysis of the features of the excimer emission revealed that it originates from pyrene dimers or higher aggregates that exist prior to excitation, as evidenced by spectral parameters compiled in Table III.^{27,28} Most revealing are the differences between the excitation spectra monitored for the monomer and the excimer emissions. While their general features are similar, the former is blue-shifted by $\Delta\lambda \approx 3$ nm, and the bands of the spectrum monitored for the excimer are broadened (Figure 6, inset). The occurrence of ground-state pyrene dimers has been detected in aqueous solutions of other labeled neutral polymers and polyelectrolytes.²⁸

Heating an aqueous solution of PNIPAM-Py-T through the LCST triggered spectral changes reported in terms of time-dependent measurements and quantum yields determinations. The average Py* monomer lifetime (τ) increased from its value in cold water, 102 ns, to 145 ns at 37 °C (Figure 7a). The change took place in a narrow temperature range encompassing the

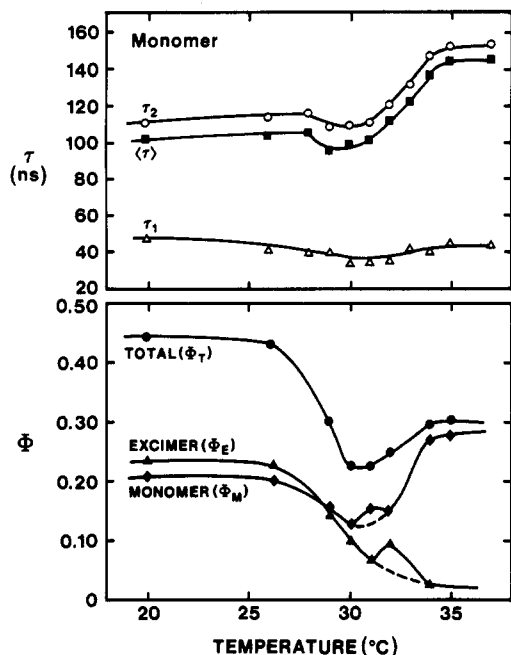


Figure 7. (a) Average pyrene monomer fluorescence lifetimes, $\langle \tau \rangle$, as a function of temperature for the same solution. Also plotted are the two components, τ_1 and τ_2 , obtained from the analysis of the fluorescence decay profiles (see text). (b) Total fluorescence quantum yields (ϕ) as a function of temperature for a solution in water of PNIPAM-Py-T (1 g L⁻¹). Also plotted are the fractional contributions of monomer (ϕ_M) and excimer (ϕ_E) emissions to that total.

solution LCST. Note that the increase in $\langle \tau \rangle$ reflects essentially that of the value of the slowest component, τ_2 . No significant changes were detected in τ_1 . Given that this component accounts for less than 10% of the total signal, one cannot rule out the possibility that the data analysis was not sensitive enough to detect minor changes in f_1 and τ_1 . The total emission quantum yield (Figure 7b) remained constant for solutions of PNIPAM-Py-T heated from 20 to *ca.* 27 °C, then it decreased to reach a minimum value (0.2) at a temperature of *ca.* 31 °C. Above this temperature ϕ , recovered an intermediate value, 0.30, which remained unaffected by further heating. The quantum yield of excimer emission decreased with increasing temperature. The onset of the drop in ϕ_E occurred at *ca.* 29 °C. The minimum value was reached at 33 °C. Curiously, a small recovery in ϕ_E took place at 31 °C, the temperature of macroscopic phase separation. Repeated measurements were performed between 29 and 32 °C to confirm that the effect was real. A small discontinuity in the monomer quantum yield temperature profile was detected also at 31 °C. Such effects were not observed while heating solutions of the singly labeled polymer PNIPAM-Py.¹⁰

Several other differences in temperature sensitivity exist between the two polymers. These are highlighted in Figure 8, which represents the temperature-induced variations of the ratios ϕ/ϕ_{20} of the temperature-dependent quantum yields (ϕ), to the quantum yields at 20 °C (ϕ_{20}) for both total emission and monomer emission. Also shown in this figure are the corresponding data for the singly labeled polymer, PNIPAM-Py. In solutions of this polymer the quantum yield of monomer emission (Figure 8, top frame) is raised by a factor of 2.5 above the LCST. This enhancement was attributed to a decrease in the extent of pyrene excimer formation and of pyrene self-quenching postulated to take place in the pyrene aggregates formed in cold aqueous solutions. The monomer quantum yield increased in solutions of PNIPAM-Py-T as well, but the effect was more modest. The overall increase amounted to less than a factor of 1.5. Moreover a significant drop of ϕ_M was observed for solutions kept between 29 and 31 °C. We interpret this pattern in terms of the occurrence of two competing temperature-induced effects: (1) a decrease in

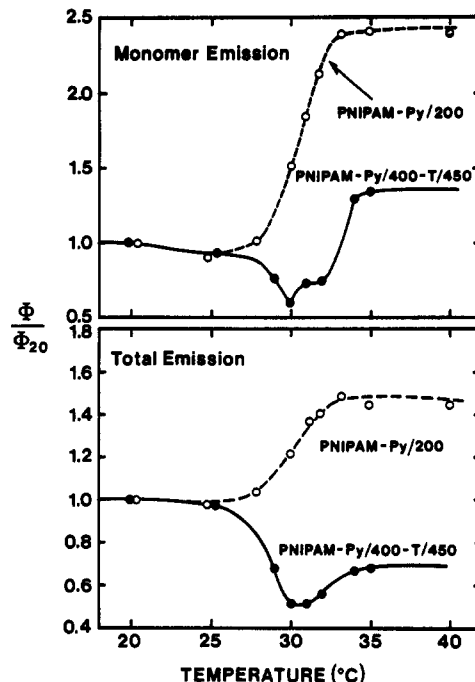


Figure 8. Plots of the ratios ϕ/ϕ_{20} of the temperature-dependent fluorescent quantum yields (Φ_F) to the fluorescence quantum yields at 20 °C (Φ_{20}) as a function of temperature for solutions of PNIPAM-Py (0.1 g L⁻¹, open circles, from ref 10) and of PNIPAM-Py-T (1 g L⁻¹, full circles) in water for the total emission (bottom frame) and the monomer emission (top frame).

TABLE IV

(a) Quantum Yields in Solutions of the Labeled Polymers

polymer	H ₂ O		MeOH		ref
	monomer	excimer	monomer	excimer	
PNIPAM-Py	0.31	0.21	0.70		10
PNIPAM-Py-T	0.41	0.04	0.03	0.01	this work

(b) Pyrene Fluorescence Lifetimes in Solutions of the Labeled Polymers

polymer	temperature	H ₂ O		MeOH		ref
		τ_1, A_1	τ_2, A_2	τ_1, A_1	τ_2, A_2	
PNIPAM-Py	25 °C	43 ns, 0.11	125 ns, 0.89	43 ns, 0.65	140 ns, 0.35	<i>a</i>
	35 °C	(τ) 116 ns	(τ) 111 ns			
PNIPAM-Py-T	25 °C	47 ns, 0.12	111 ns, 0.87	19 ns, 0.76	29 ns, 0.24	this work
	35 °C	(τ) 108 ns	(τ) 22 ns			

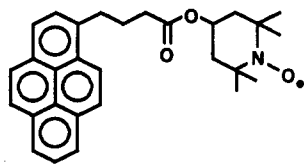
(c) Photophysical Parameters of the 1-Pyrenyl Butyrates^b

compound	quantum yield	fluorescence lifetime (ns)
Py(CH ₂) ₃ CO ₂ CH ₃	0.41	176
Py(CH ₂) ₃ CO ₂ -TEMPO (1)	0.02	3.5

^a Winnik, F. M., unpublished results. ^b Values recorded in benzene.³⁰

the efficiency of pyrene excimer formation and a reduction in the extent of pyrene self-quenching; (2) an increase in the efficiency of the quenching of Py* by the TEMPO radicals which are expected in closer contact with the fluorescent groups within the separated polymer-rich phase.

The emission of the polymer PNIPAM-Py-T in methanol was much weaker than that of the singly labeled polymer, PNIPAM-Py, for identical Py concentrations. The quantum yield of pyrene monomer emission was lower by a factor of *ca.* 20 in PNIPAM-Py-T (Table IVa). The contribution of excimers to the total emission was extremely weak ($I_E/I_M < 0.01$). Identical excitation



(1)
TEMPO-4-(1-pyrenyl)-butyrate

spectra were recorded for monomer and excimer emissions. The maxima of these spectra correspond to the wavelengths of maxima in the absorption spectrum. Therefore, the monomer and the excimer originate from the same species, Py^* in its singlet state, and its formation obeys the dynamic mechanism described by Birks.²⁹ Time-resolved measurements established that the low quantum yield was related to a shortening of the pyrene fluorescence lifetime (Table IVb). The monomer fluorescence decay curve deviated significantly from a single exponential, but a double-exponential fit was satisfactory. In this analysis the major component is a fast decaying species ($\tau = 19$ ns). The second component exhibits a slightly longer lifetime ($\tau = 29$ ns). The pyrene monomer emission of PNIPAM-Py also presents a decay curve following a biexponential law, with predominant contribution from the faster decaying species. For PNIPAM-Py though the lifetimes of both excited species are significantly longer (43 and 140 ns, respectively, Table IVb). The decreases in the pyrene fluorescence quantum yield and the shortening of its lifetime result from significant quenching of the emission by the nitroxide radicals of the EPR labels attached to the doubly labeled polymer PNIPAM-Py-T. Decreases in pyrene emission quantum yield and lifetime as a result of quenching by nitroxide radical have been detected also in solutions of compounds such as TEMPO-4-(1-pyrenyl) butyrate (1) where a pyrene group is linked to a TEMPO radical via a short alkyl chain (Table IVc).³⁰

Quenching of the Emission of PNIPAM-Py by the Nitroxide Radicals of a Free Probe (TEMPO) and of a Labeled Polymer (PNIPAM-T). *Quenching of the fluorescence of PNIPAM-Py by TEMPO.* Steady-state fluorescence spectra of the pyrene-labeled polymer PNIPAM-Py in aqueous and methanolic solutions were monitored as a function of increasing concentration of either TEMPO or PNIPAM-T. In both cases the quenching results were interpreted in terms of the Stern-Volmer model.³¹ In this treatment the fluorescence intensities I_0 and I in the absence and in the presence of quencher, respectively, are related to the quencher concentration $[Q]$ by eq 1, where K_{SV} is the Stern-

$$I_0/I = 1 + K_{SV}[Q] = 1 + k_q\tau_0[Q] \quad (1)$$

Volmer constant, k_q is the bimolecular quenching constant, and τ_0 is the lifetime of the fluorophore in the absence of quencher. Linear Stern-Volmer plots were obtained for quenching by TEMPO of the monomer and excimer emissions in methanolic solutions of PNIPAM-Py. The Stern-Volmer parameters are reported in Table V. A bimolecular quenching constant of $8.0 \times 10^9 \text{ s mol}^{-1} \text{ L}$, determined using the average monomer lifetimes (τ_0) (Table IVb) is consistent with a diffusional quenching mechanism. It agrees well with the k_q value reported for the quenching by TEMPO of pyrene fluorescence in methylcyclohexane ($8.6 \times 10^9 \text{ s}^{-1} \text{ mol}^{-1} \text{ L}$).³² Also, it is of the same order of magnitude as the value ($6.6 \times 10^9 \text{ s}^{-1} \text{ mol}^{-1} \text{ L}$) reported for the quenching by nitromethane of pyrene fluorescence in methanolic solution of PNIPAM-Py.³³

Fluorescence quenching of Py monomer and excimer by TEMPO was observed also in aqueous solutions of PNIPAM-Py, but the data did not obey the simple Stern-Volmer model. Plots of I_0/I as a function of TEMPO concentration exhibited an upward curvature, indicating an apparently more efficient quenching at higher TEMPO concentrations. In these plots two TEMPO

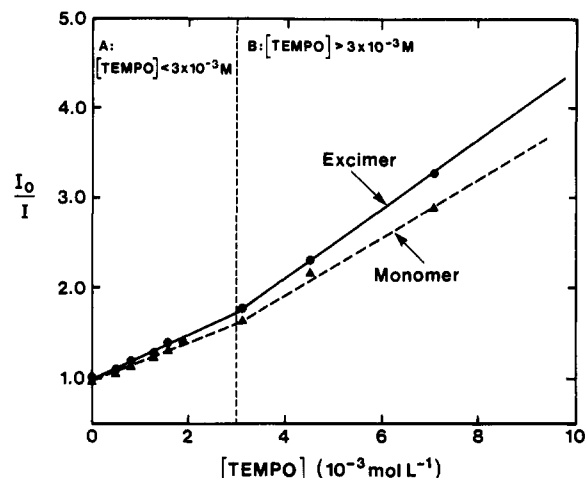


Figure 9. Ratios I_0/I of the emission intensities in the absence and in the presence of TEMPO of aqueous solutions of PNIPAM-Py (0.06 g L^{-1}) as a function of TEMPO concentration for the pyrene monomer (dotted line) and excimer (full line) emissions, 25°C , $\lambda_{\text{exc}} = 345 \text{ nm}$.

TABLE V: Quenching Data for Solutions of PNIPAM-Py and TEMPO in Methanol and in Water

solvent	monomer		excimer
	$K_{SV} (\text{mol}^{-1} \text{ L})$	$k_q (\text{s}^{-1} \text{ mol}^{-1} \text{ L})$	$K_{SV} (\text{mol}^{-1} \text{ L})$
MeOH, 25°C	890	8.0×10^9	680
water			
25°C , $[\text{TEMPO}] < 3 \times 10^{-3} \text{ mol L}^{-1}$	240	1.9×10^9	244
35°C	210	1.4×10^9	

concentration regions can be distinguished (Figure 9). For $[\text{TEMPO}] < 3 \times 10^{-3} \text{ mol L}^{-1}$, the data follow the linear Stern-Volmer model, with $K_{SV} \approx 210 \text{ mol}^{-1} \text{ L}$ for quenching of the monomer emission, a value which in combination with the averaged monomer lifetime value leads to $k_q \approx 1.9 \times 10^9 \text{ s}^{-1} \text{ mol}^{-1} \text{ L}$ for a diffusional quenching mechanism. The data corresponding to $[\text{TEMPO}] > 3 \times 10^{-3} \text{ mol L}^{-1}$ appear to follow a linear law as well, with a larger K_{SV} ($310 \text{ mol}^{-1} \text{ L}$). We postulate that in this quencher concentration domain, both dynamic and static quenching mechanisms contribute to the overall quenching, implying some form of ground-state association between TEMPO and the fluorophore. The situation presented by the TEMPO/PNIPAM-Py pair is similar to that reported for the quenching of cationic pyrenyl alkyl derivatives by a surfactant nitroxide radical.³⁴

Quenching of the fluorescence of PNIPAM-Py by PNIPAM-T: A study of the quenching of Py fluorescence in PNIPAM-Py by the TEMPO label of PNIPAM-T poses some technical difficulties, since as the TEMPO concentration increases, so does the polymer concentration. Given the low ratio of TEMPO/PNIPAM monomeric units in PNIPAM-T, extremely high polymer concentrations would be required to reach the TEMPO concentrations used in the case of the probe experiments. Nonetheless a set of experiments was carried out with solutions of constant total polymer concentration (2.5 g L^{-1}). The total polymer concentration was adjusted by addition of variable amounts of the unlabeled polymer, PNIPAM, to solutions of constant PNIPAM-Py concentration (60 ppm) and increasing amounts of PNIPAM-T. The highest TEMPO concentration thus achieved was $10^{-5} \text{ mol L}^{-1}$. Under these circumstances, no quenching of pyrene fluorescence took place in cold water, confirming the absence of interchain aggregation in cold aqueous solutions of PNIPAM. Above the LCST a small extent of quenching of the pyrene fluorescence took place (e.g., I_0/I 1.40 for $[\text{Tempo}]_{\text{label}} = 4 \times 10^{-5} \text{ mol L}^{-1}$). The separated polymer-rich phase consists of an assembly of individually coiled PNIPAM, PNIPAM-T, and PNIPAM-Py chains. Contacts between pyrene groups and

free-radical are not precluded, but they are limited by the rather high dilution of these groups in the separate polymeric phase.

Conclusion

Evidence gathered from three sources have clarified several aspects of the solution properties of hydrophobically labeled poly(*N*-isopropylacrylamides), the mechanism of the heat-induced phase transition, and the composition of the anisotropic phase formed above the cloud point. In cold water the hydrophobic dyes are associated within intrapolymeric microdomains from which the more hydrophilic TEMPO labels are essentially precluded. This point is substantiated by the low quenching efficiency of the pyrene emission by the TEMPO radicals and by the rather low sensitivity of the EPR parameters to the presence of pyrene tags along the chain. The mobility of the TEMPO radicals is slightly restricted, compared to the situation in the singly TEMPO-labeled polymer, reflecting subtle changes in the polymer dynamics, as a result of the presence of very low levels of hydrophobic substituents. When the polymer is dissolved in methanol, and hydrophobic groups do not aggregate. The macromolecule behaves as a rather flexible coil, allowing the labels to interact. Thus the local concentration of pyrene and TEMPO groups becomes high, and pyrene emission is quenched effectively by the nitroxide radicals.

The experiments also confirm that as the aqueous solutions reach their lower critical solution temperature, individual macromolecules collapse from extended chains into globules as in the case of unsubstituted poly(*N*-isopropylacrylamide).⁶ This process disrupts the hydrophobic microdomains and increases the local concentration of isolated pyrenes and TEMPO groups, thus enhancing the efficiency of fluorescence quenching. In the separated polymer-rich phase individual collapsed chains aggregate. The EPR parameters and the NMR data confirm that in this environment the probe experiences a higher microviscosity and a much reduced mobility. These initial results lead the way to general methods for monitoring the dynamics of hydrophobically modified polymers and may also provide a better understanding of the phenomena at work as stimuli-sensitive hydrogels undergo their phase transition.

Acknowledgment. S.H.B, W.P., M.G.-G., and N.J.T. thank the National Science Foundation for their generous support of this research.

References and Notes

(1) Hoffman, A. S. *J. Controlled Release* **1986**, *4*, 213. Okano, T.; Bae, Y. H.; Kim, S. W. *J. Controlled Release* **1990**, *11*, 255. Wu, X. S.; Hoffman, A. S.; Yager, P. *J. Intelligent Mater. Syst. Struct.* **1993**, *4*, 202.

(2) Feil, H.; Bae, Y. H.; Feijen, J.; Kim, S. W. *J. Membr. Sci.* **1991**, *64*, 283. Galaev, I. Y.; Mattiasson, B. *Enzyme Microb. Technol.* **1993**, *15*, 354.
 (3) Guenet, J.-M. *Thermoreversible Gelation of Polymers and Biopolymers*, Academic Press: San Diego, CA, 1992.
 (4) Heskins, M.; Guillet, J. E. *J. Macromol. Sci., Chem.* **1968**, *A2*, 1441.
 (5) Schild, H. G.; Tirrell, D. A. *J. Phys. Chem.* **1990**, *94*, 4352.
 (6) Kubota, K.; Fujishige, S.; Ando, I. *J. Phys. Chem.* **1990**, *94*, 5154. Inomata, H.; Yagi, Y.; Otake, K.; Konno, M.; Saito, S. *Macromolecules* **1989**, *22*, 3494. Yamamoto, I.; Iwasaki, K.; Hirotsu, S. *J. Phys. Soc. Jpn.* **1989**, *58*, 210.
 (7) Winnik, F. M. *Polymer* **1990**, 2125.
 (8) Schild, H. G.; Tirrell, D. A. *Macromolecules* **1992**, *25*, 4553.
 (9) Ohta, H.; Ando, I.; Fujishige, S.; Kubota, K. *J. Mol. Struct.* **1991**, *245*, 391.
 (10) Winnik, F. M. *Macromolecules* **1990**, *23*, 233.
 (11) Winnik, F. M.; Ottaviani, M. F.; Bossmann, S. H.; Garcia-Garibay, M.; Turro, N. J. *Macromolecules* **1992**, *25*, 6007.
 (12) Winnik, F. M.; Ottaviani, M. F.; Bossmann, S. H.; Pan, W.; Garcia-Garibay, M.; Turro, N. J. *Macromolecules*, in press.
 (13) Birks, J. B. *Photophysics of Aromatic Molecules*; John Wiley: New York, 1970.
 (14) Green, S. A.; Simpson, D. J.; Zhou, G.; Ho, P. S.; Blough, N. V. *J. Am. Chem. Soc.* **1990**, *112*, 7337.
 (15) London, E. *Mol. Cell. Biochem.* **1982**, *45*, 181. Winiski, A. P.; Eisenberg, M.; Langner, M.; McLaughlin, S. *Biochemistry* **1988**, *27*, 386.
 (16) Atik, S. S.; Singer, L. A. *J. Am. Chem. Soc.* **1978**, *100*, 3234. Scaiano, J. C.; Paraskevopoulos, C. *Can. J. Chem.* **1984**, *62*, 2351.
 (17) Matko, J.; Ohki, K.; Edidin, M. *Biochemistry* **1992**, *31*, 703-711.
 (18) Browning, J. L.; Nelson, D. L. *J. Membrane Biol.* **1979**, *49*, 75. Winnik, F. M. *Polymer* **1990**, *31*, 2125.
 (19) Winnik, F. M. *Macromolecules* **1987**, *20*, 2745.
 (20) Fujishige, S. *Polymer J.* **1987**, *19*, 297.
 (21) Schneider, D. J.; Freed, J. H. In *Biological Magnetic Resonance*; Berliner, L. J., Teuben, J., Eds.; Plenum Press: New York, 1989; Vol. 8, pp 1-76.
 (22) Turro, N. J. *Modern Molecular Photochemistry*; The Benjamin/Cummings Publishing Co.: Menlo Park, A, 1978; p 117.
 (23) Melhuish, W. H. *J. Phys. Chem.* **1961**, *65*, 229.
 (24) Ibbett, R. N.; Philp, K.; Price, D. M. *Polymer* **1992**, *33*, 4087.
 (25) Orrell, K. G. In *Annual Reports of NMR Spectroscopy*; Webb, G. A., Ed.; Academic Press: London, 1979; pp 1-123.
 (26) Miller, W. G. In *Spin Labeling II: Theory and Applications*; Berliner, L. J., Ed.; Academic Press: New York, 1979; p 173.
 (27) The parameters are (a) the wavelength λ_E of maximum of excimer emission, (b) the ratio I_E/I_M of the intensity of the excimer emission to that of the monomer emission, (c) P_M , the peak-to-valley ratio of the (0,0) transition in 1L_a band in the excitation spectrum viewed at 396 nm, and (d) P_E , the peak-to-valley ratio of the (0,0) transition in 1L_a band in the excitation spectrum viewed at 480 nm.
 (28) Winnik, F. M. *Chem. Rev.* **1993**, *93*, 587.
 (29) Birks, J. B. *Rep. Prog. Phys.* **1975**, *38*, 903.
 (30) Turro, N. J.; Malinowski, M. D.; Lipson, M., unpublished results.
 (31) Lakowicz, J. R. *Principles of Fluorescence Spectroscopy*; Plenum Press: New York, 1983.
 (32) Watkins, A. R. *Chem. Phys. Lett.* **1974**, *29*, 527.
 (33) Winnik, F. M. *Macromolecules* **1990**, *23*, 1647.
 (34) Atik, S. S.; Kwan, C. L.; Singer, L. A. *J. Am. Chem. Soc.* **1979**, *101*, 5696.